Terahertz spectroscopy of Ni–Ti alloy thin films

A. D. Jameson,[1] J. W. Kevek,[1] J. L. Tomaino,[1] M. Hemphill-Johnston,[2] M. J. Paul,[2] M. Koretsky,[2] E. D. Minot,[2] and Yun-Shik Lee[2,a)]
[1]*Department of Physics, Oregon State University, Corvallis, Oregon 97331-6507, USA*
[2]*School of Chemical, Biological & Environmental Engineering, Oregon State University, Corvallis, Oregon 97331, USA*

(Received 1 April 2011; accepted 11 May 2011; published online 3 June 2011)

We investigate the carrier dynamics in nickel–titanium (Ni–Ti) alloy thin films using terahertz transmission spectroscopy. Analyzing the power transmission data and the transmitted waveforms, we obtained the alloy resistivity as a function of Ti concentration. Sharp changes in the resistivity were observed at the Ti fractions of 22%, 44%, and 62%, indicating that structural disorder is greatly enhanced when the alloy undergoes a phase transition. © *2011 American Institute of Physics*. [doi:10.1063/1.3596456]

Nickel–titanium (Ni–Ti) alloys have exotic mechanical and electromechanical properties such as shape memory effect, superelasticity, and electroplasticity.[1–4] Resembling the deformation behavior of biological materials, the excellent mechanical properties of Ni–Ti alloys make them useful for medical devices including orthopedic implants, orthodontic archwires, and various interventional devices.[5,6] Ni–Ti alloys also have the potential for applications in microelectromechanical systems.[7–10] With the advance of Ni–Ti thin-film manufacturing technologies and nanoscale characterization techniques, the micromechanical properties have been rigorously studied in recent years.[11–15]

In this letter, we present experimental measurements of the resistivity of Ni–Ti thin films obtained via terahertz (THz) imaging and spectroscopy. It has been reported that electrical conductivity is a good property for characterizing phase transitions and mechanical properties of bulk Ni–Ti alloys,[16] yet the electrical transport properties of thin films are unexplored at present. THz spectroscopy has proven to be an outstanding way to nondestructively examine the electrical properties of thin metal films.[17,18] Furthermore, THz imaging can assess local resistivity on the scale of 100 μm in a free space arrangement,[19] and the spatial resolution can be improved to a sub-10 μm scale with near-field capability.[20]

Figure 1 illustrates the experimental scheme for THz transmission measurements of a Ni–Ti film. The Ni–Ti film was deposited on an intrinsic Si substrate by Ar plasma sputtering. We prepared several samples of varying thickness (30–120 nm) and Ti concentration (0%–100%). The samples were not annealed, and hence the structure of the Ni–Ti films was amorphous.[11] The alloy composition of each sample was determined by energy-dispersive x-ray spectroscopy (EDX). Half of each sample surface remains bare for side-by-side comparison between THz transmissions of Ni–Ti-on-Si and bare Si. We measured the film thickness (d) with atomic force microscopy (AFM). The AFM cross-section of a sample (Ti, 29%) shown in Fig. 1 measures its thickness (d=80.5 nm), and also shows that the sample surface is spatially uniform beyond 10 μm from the edge. We carried out THz transmission spectroscopy of the samples using broadband THz pulses. The THz pulses were generated by optical rectification of femtosecond laser pulses in a 1 mm ZnTe crystal. The light source was a 1 kHz Ti:sapphire amplifier producing 800 nm femtosecond pulses (pulse energy, 1 mJ; pulse duration, 90 fs). THz pulses were focused onto the Ni–Ti/Si sample or the bare Si substrate with a beam size of 0.5 mm. The transmitted THz pulses were measured by either a L-He-cooled Si:bolometer (sensitive to time-averaged THz power) or by electro-optic (EO) sampling using a 1 mm ZnTe crystal.

Figure 2 shows a transmission image of 30 nm and 90 nm Ni–Ti films (20% Ti) obtained by raster scanning with the Si-bolometer. The pixel size is 0.4 mm and data were acquired with a 100 ms pixel integration time. Each sample was mounted on a metal plate with a circular hole (5 mm diameter). The uniform transmission indicates that the sample is spatially homogeneous in the macroscopic scale.

Figure 3(a) shows the THz waveforms directly transmitted, i.e., with no internal reflection, through the alloy films of several different Ti concentrations from 0% to 51%. The corresponding relative transmission spectra (ratio of the transmission through Ni–Ti-on-Si to that of bare Si) are shown in Fig. 3(b). The spectral responses are flat in the THz region. The general trend in this figure is that the THz transmission

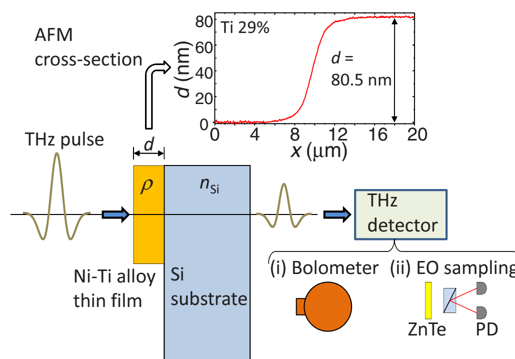

FIG. 1. (Color online) Experimental scheme for THz transmission measurement of a Ni–Ti thin film on a Si substrate. Half of each sample surface remains bare for side-by-side comparison between Ni–Ti-on-Si and bare Si. The film thickness (d) is measured by AFM. An AFM measurement shows the cross-section of a Ni–Ti (71%–29%) film (d=80.5 nm). Broadband THz pulses transmitted through the sample are detected by a bolometer or electro-optic sampling.

[a)]Electronic mail: leeys@physics.oregonstate.edu.

 © 2011 American Institute of Physics

Downloaded 07 Jul 2011 to 128.193.96.87. Redistribution subject to AIP license or copyright; see http://apl.aip.org/about/rights_and_permissions

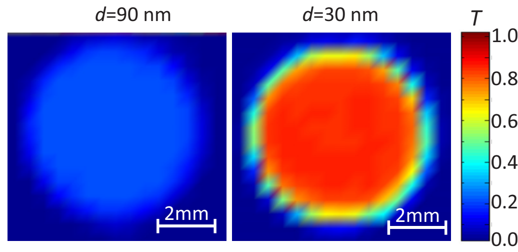

FIG. 2. (Color online) THz transmission image (pixel size is 0.4 mm) of 30 nm and 90 nm Ni–Ti film (Ti, 20%) deposited on a Si substrate acquired by raster scanning with broadband THz pulses and a Si:bolometer.

monotonically increases as the Ti concentration increases, yet more detailed measurements reveal far more complex dependence on the Ti concentration, which will be shown in Fig. 4.

We analyzed the THz power transmission data and the transmitted THz waveforms using thin-film Fresnel coefficients and the Drude model. The alloy layer is treated as an optically thin conductive film ($d \ll \delta_{\mathrm{THz}}$, skin depth), whereas the Si substrate is considered an optically thick dielectric medium. The ratio of skin depth to film thickness of the samples ranges from 3.3 (Ti, 0%) to 17 (Ti, 24%) at 1 THz. The substantial thinness of the samples compared with their skin depths validates the thin-film premise. In this picture, the transmitted THz waveform is an exponentially decaying and periodic pulse train due to multiple reflections within the substrate, which was experimentally confirmed by THz time-domain spectroscopy. In this simple model, THz transmission is solely determined by the alloy resistivity. The ratio of

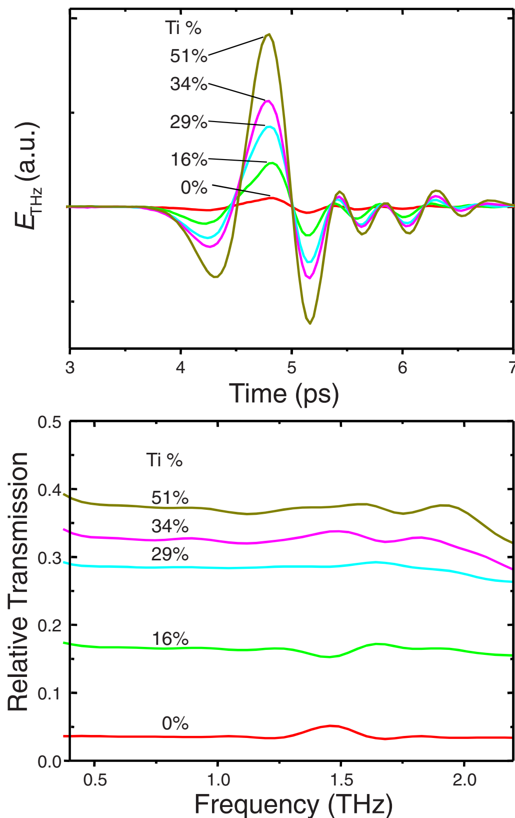

FIG. 3. (Color online) (a) THz waveforms transmitted through Ni–Ti alloy films and (b) corresponding relative transmission spectra. The Ti concentrations (thickness) of the samples are 0.0% (68.9 nm), 16.2% (72.0 nm), 28.8% (80.5 nm), 34.4% (82.3 nm), and 51.4% (77.7 nm).

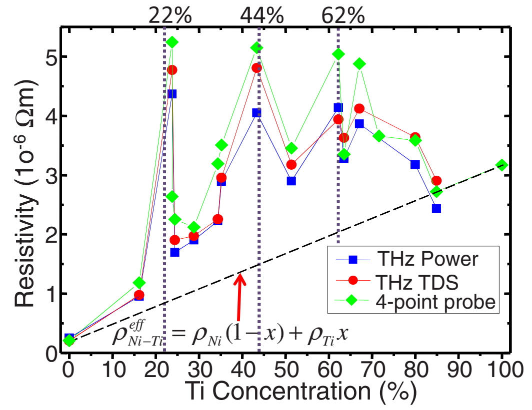

FIG. 4. (Color online) Ni–Ti alloy resistivity calculated from the power transmission (square) and transmitted waveforms (circle) as a function of Ti concentration. The four-point probe results (diamond) are also shown for comparison. The Ti concentrations (thickness) of the Ni–Ti thin-film samples are 0.0% (68.9 nm), 16.2% (72.0 nm), 23.8% (63.92 nm), 24.4% (70.97 nm), 28.8% (80.5 nm), 34.4% (82.3 nm), 35.2% (72.17 nm), 43.4% (70.2 nm), 51.4% (77.7 nm), 62.2% (68.5 nm), 63.5% (59.3 nm), 67.1% (71.4 nm), 80.0% (64.5 nm), and 84.9% (63.2 nm). The dashed line depicts the mean resistivity of the effective medium. The vertical dotted lines indicate the Ti concentrations of 22%, 44%, and 62%, at which phase transitions occur at the growth temperature.

the total transmission of Ni–Ti-on-Si to that of bare Si is a function of the Ni–Ti resistivity, ρ, and is expressed as

$$T_{rel}(\rho) = \left|\frac{t(\rho)}{t_{13}}\right|^2 \frac{1-|r_{34}r_{31}|^2}{1-|r_{34}r(\rho)|^2}, \qquad (1)$$

where $t_{ij}=2n_i/(n_i+n_j)$ and $r_{ij}=(n_i-n_j)/(n_i+n_j)$ are the Frensnel coefficients with the refractive indices of air ($n_1=n_4=1$) and Si ($n_3=3.42$).[19] The transmission and internal reflection coefficients of the Ni–Ti/Si interface, $t(\rho)$ and $r(\rho)$, are given as

$$t(\rho) = \frac{2\rho}{(n_3+1)\rho + Z_0 d}, \qquad (2)$$

$$r(\rho) = \frac{(n_3-1)\rho - Z_0 d}{(n_3+1)\rho + Z_0 d}, \qquad (3)$$

where $Z_0(=376.7\ \Omega)$ is the vacuum impedance.[19] These thin-film formulas, Eqs. (1)–(3), are valid because the Ni–Ti films are substantially thinner (60–80 nm) than the skin depth (230–1100 nm at 1 THz). The relative transmission of the directly transmitted THz pulses (e.g., Fig. 3) is expressed as $t_{rel}=t(\rho)/t_{13}$. It is notable that the spectral response is flat in this Drude picture.

As a result of this analysis, we obtained the alloy resistivity as a function of Ti concentration as shown in Fig. 4. The resistivity was calculated from the results of two different measurements: THz power transmission (solid square) and transmitted THz waveforms (solid circle). We also measured dc resistivity using four-point contact probes, and the result is shown for comparison (solid diamond). The results of these three independent measurements are in a good agreement. We note that THz spectroscopy is a nondestructive method to probe the thin films while the dc conductivity measurements damage the sample surfaces. Furthermore, THz imaging measures local resistivity on the scale of 0.1 nm.

Downloaded 07 Jul 2011 to 128.193.96.87. Redistribution subject to AIP license or copyright; see http://apl.aip.org/about/rights_and_permissions

A phenomenological model based on the effective medium theory is useful to describe the alloy resistivity

$$\rho_{\text{Ni–Ti}} = \rho^{eff}_{\text{Ni–Ti}} + \Delta\rho. \qquad (4)$$

Assuming the Drude model, i.e., that the resistivity is proportional to the scattering time, we can express the mean resistivity of the Ni and Ti effective medium as $\rho^{eff}_{\text{Ni–Ti}} = \rho_{\text{Ni}}(1-x) + \rho_{\text{Ti}}x$, where x is the Ti concentration. The large deviation $\Delta\rho$ of the measured alloy resistivity from $\rho^{eff}_{\text{Ni–Ti}}$ indicates that the carrier scattering rate is significantly higher in the Ni–Ti mixtures than in a single-element material.[21] This reflects the structural disorder in the Ni–Ti alloys. A remarkable feature of the data is the sharp changes in the resistivity which occur near the Ti concentrations of 22%, 44%, and 62%. It has been reported that the alloy undergoes a phase transition at each of these compositions at room temperature.[22] We speculate that the structural disorder in the alloy thin films is largely enhanced near the phase-transition concentrations giving rise to the resistivity increases.

In conclusion, we have systematically studied the Ti-concentration dependent electrical resistivity of Ni–Ti alloy films using THz transmission spectroscopy as a nondestructive evaluation method. The measured resistivity shows distinctive peaks at the Ti concentrations of 22%, 44%, and 62% where the phase transitions occur. The results imply that the alloy films undergo significant structural disordering near the phase-transition concentrations.

This work is supported by National Science Foundation and Oregon Nanoscience and Microtechnologies Institute.

[1]W. J. Buehler, J. V. Gilfrich, and R. C. Wiley, J. Appl. Phys. **34**, 1475 (1963).
[2]F. E. Wang, W. J. Buehler, and S. J. Pickart, J. Appl. Phys. **36**, 3232 (1965).
[3]C. M. Wayman, I. Cornelis, and K. Shimizu, Metall. Trans. **6**, 115 (1972).
[4]T. Honma and H. Takei, J. Jpn. Inst. Met. **39**, 175 (1975).
[5]Professional Engineering Publishers, *Medical Applications for Shape-Memory Alloys (SMA)* (Wiley, Germany, 1999).
[6]I. P. Lipscomb and L. D. M. Nokes, *The Application of Shape Memory Alloys in Medicine* (Wiley, Germany, 1996).
[7]J. L. Seguin, M. Bendahan, A. Isalgue, V. Esteve-Cano, H. Carchano, and V. Torra, Sens. Actuators, A **74**, 65 (1999).
[8]W. Ni, Y. Cheng, and D. S. Grummon, Appl. Phys. Lett. **82**, 2811 (2003).
[9]A. Camposeo, F. Fuso, M. Allegrini, E. Arimondo, and A. Tuissi, Appl. Phys. A: Mater. Sci. Process. **79**, 1141 (2004).
[10]H. Lee and A. G. Ramirez, Appl. Phys. Lett. **85**, 1146 (2004).
[11]J. D. Busch, A. D. Johnson, C. H. Lee, and D. A. Stevenson, J. Appl. Phys. **68**, 6224 (1990).
[12]D. Z. Xie, B. K. A. Ngoi, A. S. Ong, Y. Q. Fu, and B. H. Lim, Nucl. Instrum. Methods Phys. Res. B **211**, 363 (2003).
[13]Y. Zhang, Y. Cheng, and D. S. Grummon, Appl. Phys. Lett. **89**, 041912 (2006).
[14]X. Wang, Y. Bellouard, Z. Xue, and J. J. Vlassak, Appl. Phys. A: Mater. Sci. Process. **90**, 689 (2008).
[15]X. Huang and A. G. Ramirez, Appl. Phys. Lett. **95**, 101903 (2009).
[16]H. Matsumoto, J. Alloys Compd. **364**, 132 (2004).
[17]M. Walther, D. G. Cooke, C. Sherstan, M. Hajar, M. R. Freeman, and F. A. Hegmann, Phys. Rev. B **76**, 125408 (2007).
[18]N. Laman and D. Grischkowsky, Appl. Phys. Lett. **93**, 051105 (2008).
[19]J. L. Tomaino, A. D. Jameson, J. W. Kevek, M. J. Paul, A. M. van der Zande, R. A. Barton, P. L. McEuen, E. D. Minot, and Y. Lee, Opt. Express **19**, 141 (2011).
[20]K. Ishihara, K. Ohashi, T. Ikari, H. Minamide, H. Yokoyama, J. Shikata, and H. Ito, Appl. Phys. Lett. **89**, 201120 (2006).
[21]A. Fert and I. A. Campbell, Phys. Rev. Lett. **21**, 1190 (1968).
[22]*Binary Alloy Phase Diagrams*, 2nd ed., edited by T. B. Massalski (ASM International, Metals Park, OH, 1990).

Downloaded 07 Jul 2011 to 128.193.96.87. Redistribution subject to AIP license or copyright; see http://apl.aip.org/about/rights_and_permissions